DIVERTOR HEAT AND PARTICLE FLUX DUE TO ELMs IN DIII–D AND ASDEX-UPGRADE

by
A.W. LEONARD, W. SUTTROP, T.H. OSBORNE, T.E. EVANS,
D.N. HILL, A. HERMANN, C.J. LASNIER, D.M. THOMAS,
J.G. WATKINS, W.P. WEST, M. WEINLICH, and H. ZOHM

DIVERTOR HEAT AND PARTICLE FLUX DUE TO ELMs IN DIII–D AND ASDEX-UPGRADE

by
A.W. LEONARD, W. SUTTROP,[†] T.H. OSBORNE, T.E. EVANS,
D.N. HILL,[‡] A. HERMANN,[†] C.J. LASNIER,[‡] D.M. THOMAS,
J.G. WATKINS,[◊] W.P. WEST, M. WEINLICH,[†] and H. ZOHM[†]

[†]Max Planck Institute for Plasma Physics
[‡]Lawrence Livermore National Laboratory
[◊]Sandia National Laboratories, Albuquerque

ABSTRACT

We characterize the divertor target plate heat and particle fluxes that occur due to Edge-Localized-Modes (ELMs) during H–mode in DIII–D and ASDEX-Upgrade. During steady-state ELMing H–mode the fraction of main plasma stored energy lost with each ELM varies from 6% to 2% as input power increases above the H–mode power threshold. The ELM energy is deposited near the strikepoints on the divertor target plates in a fast time scale of ≤ 1 ms. The spatial profile of the ELM heat pulse is flatter and broader, up to about a factor of 2, than that of the heat flux between ELMs. On ASDEX-Upgrade the inboard strike-point receives the greatest fraction, $\geq 75\%$, of ELM divertor heat flux, while on DIII–D the in/out split is nearly equal. The toroidal asymmetry of the heat pulse has produced a peaking factor on DIII–D of no more than 1.5. The particle flux, as measured by Langmuir probes, has also been found to be localized near the divertor strike-points. The increased particle flux during ELMs is a significant fraction of the total time-integrated divertor plate particle flux.

1. INTRODUCTION

Steady-state operation of H–mode in a tokamak currently relies on Edge-Localized Modes (ELMs) to relieve the plasma pressure gradient that builds just inside the separatrix [1]. Type I giant ELMs are most common and occur when the edge pressure gradient is near the ideal ballooning limit and are believed to be triggered by a ballooning instability [2]. An ELM event is characterized by a burst of H_α, a fast drop in plasma density and temperature just inside the separatrix, and a burst of particles and heat flux at the divertor target plate [3].

A characterization of divertor fluxes due to ELMs is important in the design of future divertor tokamaks. Long pulse, high power tokamaks, such as ITER, require careful design to handle the high divertor power. ELMs represent a transient that may circumvent methods of heat flux control and produce a significant amount of divertor target erosion [4]. Secondly future divertors may be strongly baffled to control neutral particle recycling. If ELMs produce a significant flux of particles with a different spatial distribution than the steady flux, then that profile must be factored into the design. Finally, it is important to measure the ELM fluxes to accurately model divertor plasmas. Divertor modeling is currently based on divertor measurements that are either measured between ELMs or averaged over them. These factors must be taken into account to get a realistic model of divertor plasma behavior.

We will first discuss the energy loss from the main plasma due to ELMs in Section 2, producing a scaling relation that takes into account the different parameters of DIII–D and ASDEX-Upgrade. Section 3 will present divertor plate heat fluxes due to ELMs with particle fluxes presented in Section 4. Finally, in Section 5 we will summarize the results and discuss implications for ITER.

2. CORE PLASMA ENERGY LOSS

For this study ELM measurements were made in single null plasmas during the steady state phase of ELMing H–mode. On ASDEX-Upgrade an input power scan of 4–8 MW was performed on plasmas with a current of 1.0 MA, a toroidal field of 2.5 T, q_{95} of 3.9 and an average density of $7 \times 10^{13} \text{cm}^{-3}$. These conditions produced a steady-state H–mode with regular Type I ELMs. The frequency of the ELMs scaled linearly with the input power from 77 Hz at 4 MW to 200 Hz at 8 MW of input power. Over this range of input power the energy lost per ELM, determined from magnetic equilibrium measurements, remained nearly constant at 16.9 kJ $\pm$ 5.5 kJ. The uncertainty or variation in these and other ELM measurements results from a combination of variation in ELM amplitude and diagnostic instrumental noise. The linear scaling of ELM frequency and constant energy per ELM results in a nearly constant fraction of the input power, typically 30% for Type I ELMs, being carried across the separatrix by ELMs on ASDEX-Upgrade.

On DIII–D, power was varied from 2.5 MW to 12.0 MW at plasma currents of 1.0, 1.4 and 1.8 MA at a toroidal field of 2.1 T for a q_{95} variation of 6.4 to 3.6. The main plasma average density during the steady-state H–mode phase varied from $5 \times 10^{13} \text{cm}^{-3}$ at 1.0 MA to $9 \times 10^{13} \text{cm}^{-3}$ at 1.8 MA. Loss of energy per ELM on DIII–D is determined from diamagnetism measurements. On DIII–D there are large variations in ELM magnitude at these parameters. Small ELMs, associated with internal plasma relaxations, carry negligible energy across the separatrix and are not counted. Over this parameter regime the energy loss per ELM can vary from about 20 kJ to 70 kJ with a frequency proportional to injected power. Roughly, the energy loss per ELM is constant with injected power and increases with plasma current.

The data from DIII–D and ASDEX-Upgrade can be compared by analyzing the fraction of main plasma energy lost by each ELM. In Fig. 1 we plot the fractional ELM energy loss versus the input power normalized by a parameter related to the expected H–mode power threshold [5]. For an H–mode threshold parameter we use the toroidal field B_t times the plasma surface area, S. We have removed the uncertain density dependence from the standard scaling because, for among other reasons, this scaling applies to the density before the H–mode transition not the density attained after it. The data indicates that the greater the input power is above the H–mode power threshold the smaller the fraction of main plasma energy that is lost at each ELM. The data from DIII–D and ASDEX-Upgrade can be seen to follow the same trend with 2%–6% of the plasma energy lost with each ELM.
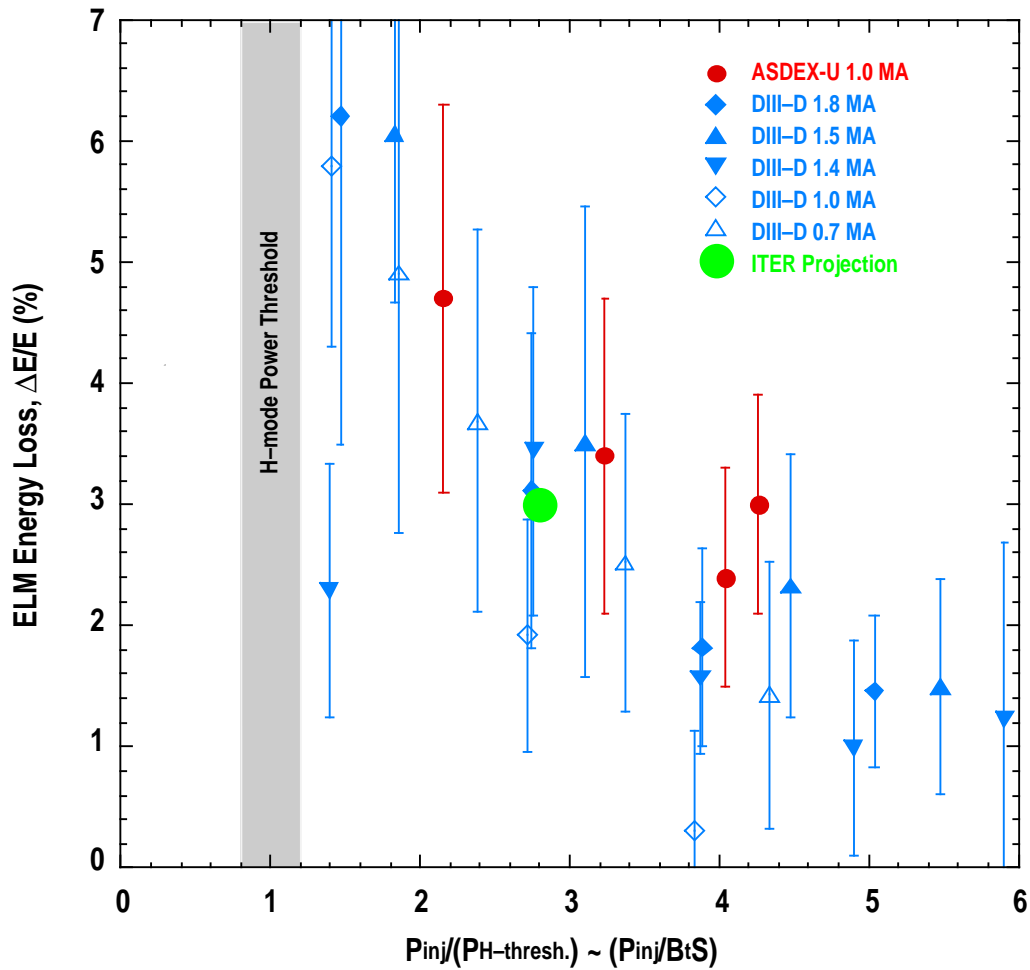
Fig. 1. The fraction of main plasma stored energy lost with an individual ELM is plotted vs the injected power normalized by a parameter related to the H–mode power threshold. The normalization parameter is $B_t, {}^*S$, the toroidal field times the plasma surface area.

3. DIVERTOR HEAT FLUX

The divertor target energy flux due to ELMs is inferred from IR surface temperature measurements on both ASDEX-Upgrade [6] and DIII–D [7]. The ELM heat flux typically lasts less than 1 ms on both tokamaks. The time response of the IR systems is ~120 µs, which is fast enough to resolve the energy flux contribution from individual ELMs as the ELM energy is typically deposited on the divertor target in the order of a few hundred microseconds. However, this time response is insufficient to resolve faster temporal details of a single ELM which may occur in 100 µs or less. Further complicating the interpretation of the fast IR measurements is the observed existence of a thin amorphous layer of graphite covering the divertor target [8] and changing the surface thermal characteristics of the graphite tiles. This is particularly important in the interpretation of fast heat pulses and has been taken into account in the data analysis, but it still represents an uncertainty in the magnitude of the ELM heat flux. Uncertainty in the integrated divertor ELM energy can be reduced by taking into account total deposited energy constraints. On DIII–D, with its video based IR temperature measurements it is more difficult to apply this energy constraint and results in a greater systematic uncertainty of ~30% for DIII–D ELM divertor energy fluxes.

The profiles of integrated ELM energy flux and associated steady state heat fluxes are shown for ASDEX-Upgrade in Fig. 2(a) and DIII–D in Fig. 2(b). The heat flux profiles from the two tokamaks show several common features. The ELM energy flux is localized to the strikepoint region, with the peak a few centimeters outside the separatrix and the profile fairly flat over the SOL region. The profile of individual ELMs exhibit more structure with secondary peaks varying 20%–30% from ELM to ELM. The profile irregularities average out over many ELMs to produce a flatter profile. It is difficult to quantify the width of the ELM energy profile, but typically most of the energy falls within a width of about 2 to 3 e-folding lengths of the quiescent profile. At the outer strikepoint ELMs make only a small contribution to the total heat flux. At the inboard strike-point, however, the ELM energy flux accounts for ≥90% of the total heat flux to the inboard divertor on both tokamaks. The remaining heat flux due to the steady period between ELMs lies within the uncertainty of the measurement. Typically during ELMing H–mode on DIII–D and ASDEX-Upgrade the inboard divertor plasma is detached from the target plate resulting in very low heat flux between ELMs, even with no gas puffing and an attached outer divertor. After accounting for flux expansion the inboard divertor ELM profile is similar to the outboard.
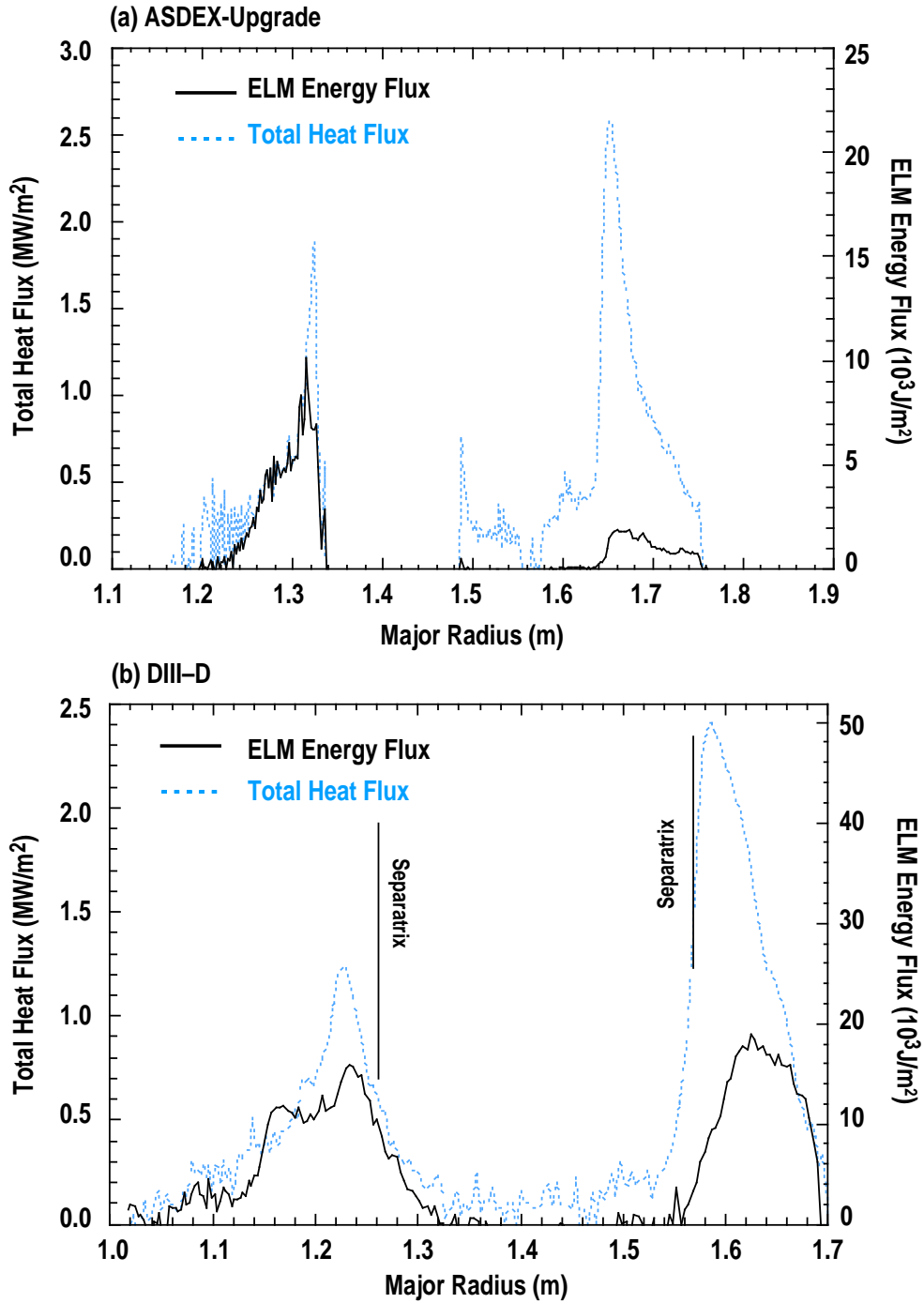
(a) ASDEX-Upgrade

(b) DIII–D

Fig. 2.   The ELM energy flux and steady state heat flux profiles for a) ASDEX-Upgrade and b) DIII–D. The heat flux profiles, read on the left scale, are the total average heat flux profiles without subtracting ELMs and the heat flux due to ELMs above the steady-state heat flux level. The ELM profile is averaged over many ELMs in a single discharge. Dividing the left scale by the ELM frequency produces the right scale where the ELM profiles can be read as an energy flux per ELM.

One apparent difference between the ASDEX-Upgrade and DIII–D data is the in/out ratio of the ELM energy flux. On ASDEX-Upgrade the ELM flux is heavily weighted to the inboard divertor while on DIII–D the balance is nearly equal with the outboard ELM energy flux ~90% of the inboard. The ELM divertor power can be calculated by integrating over the profile, summing up contributions from individual ELMs and dividing by the time of analysis. On ASDEX-Upgrade 11% of the injected power arrives as ELM heat flux to the inboard divertor and 4% to the outboard. This compares to 25% of the injected power that arrives to the outboard divertor as steady heat flux between ELMs and negligible steady heat flux to the inboard. The total divertor ELM energy flux, ~15% of the injected power, accounts for 50% of the ELM losses from the main plasma as measured by the magnetics. A significant fraction of the ELM loss may leave as radiation, but this was not measurable on ASDEX-Upgrade because of the time response of the bolometer system.

On DIII–D the inboard divertor ELM energy flux accounts for ~11% of the injected power and the outboard ~10%. The greater outboard ELM flux also results in a greater fraction of the ELM energy loss deposited on the divertor plates on DIII–D than ASDEX-Upgrade. On DIII–D half to all of the main plasma energy loss measured by diamagnetism is deposited on the divertor plates as heat flux. Bolometric measurements on DIII–D indicate that ≤15% of the ELM energy is radiated away, mostly in the divertor. The scatter in energy accountability, 50%–100%, may be in large part due to measurement limitations.

Another concern is the toroidal symmetry of the deposited ELM energy. If the ELM energy is concentrated in one toroidal location much greater divertor plate erosion can occur. On DIII–D two IR cameras were employed to simultaneously observe individual ELMs at two toroidal locations separated by 105°. In Fig. 3 the total deposited energy for individual ELMs observed by the first camera is plotted versus the energy measured by the second camera. A fit through the center of the distribution has a slope ~1 indicating the cameras are similarly calibrated. The edges of the distribution highlight the scatter in the data which results from a combination of toroidal asymmetries and instrumental noise. This data indicates that the toroidal peaking factor is usually less than 1.5 when integrated over the entire ELM heat flux. Previous measurements of divertor tile currents on DIII–D [9] have shown greater toroidal asymmetry than this, but on a faster timescale. If the limiting time scale for energy deposition to produce erosion is found to be significantly faster than 100 μs then faster IR measurements will be needed to better characterize the ELM energy flux.
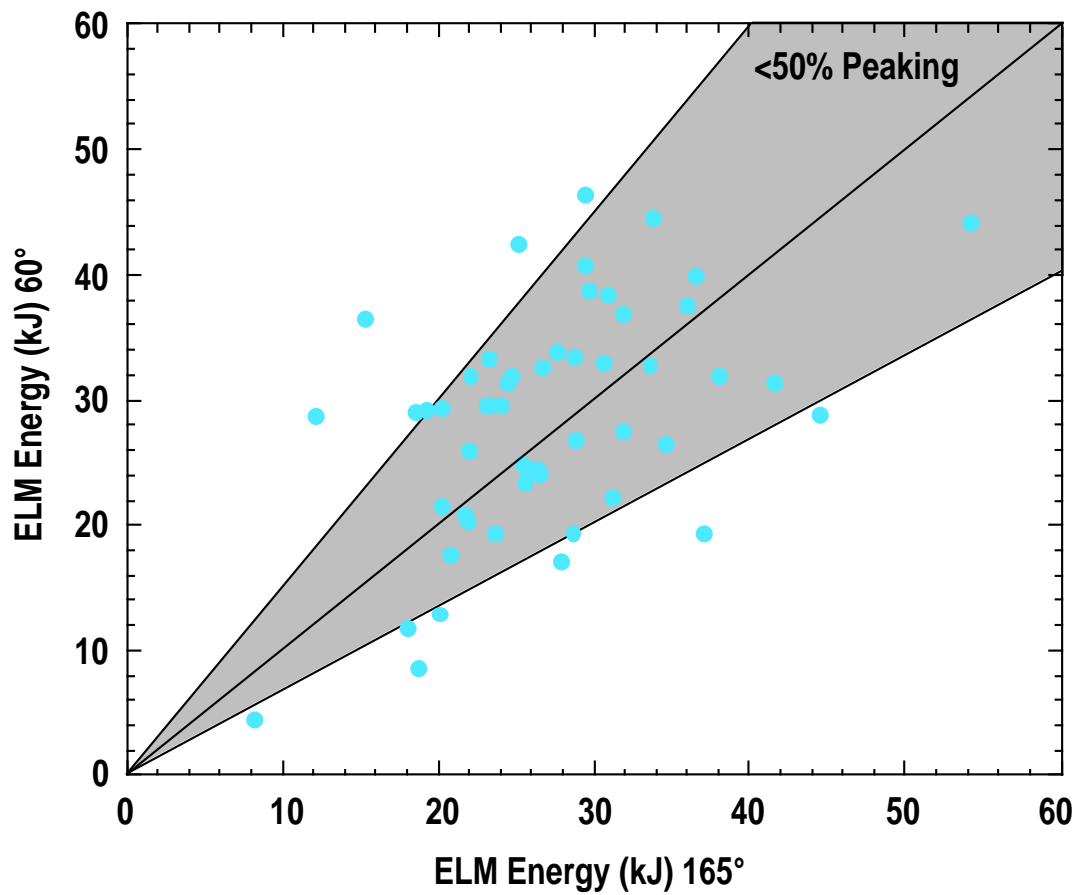
Fig. 3. The energy of individual ELMs as measured by two IR cameras separated toroidally 100° The scatter in the data is due to possible toroidal asymmetries in combination with inherent error in the measurement. The boundaries drawn are those consistent with a toroidal peaking factor of ≤ 1.5.

4. DIVERTOR PARTICLE FLUX

The divertor plate particle fluxes due to ELMs are also important for future divertor designs that may be highly baffled. If an ELM causes significant particle flux to regions far outside the separatrix this must be designed into the baffling structure. Information about particle flux can be obtained from H_α measurements, but quantitative interpretation can be problematic. Particle fluxes can be measured as saturation current with Langmuir probes. On the ASDEX-Upgrade divertor triple probes are used to obtain particle flux, while on DIII–D a divertor array of single probes biased into saturation are used. Particle flux measurements during ELMing H–mode for one discharge from the two tokamaks are summarized in Fig. 4, and present similar conclusions. The particle flux profile during the quiescent period between ELMs is seen to peak near the separatrix with a spatial width similar to the heat flux. During an ELM the instantaneous particle flux can increase a factor of 10–50, but only for a short time. Because of the short ELM duration the time-averaged particle flux due to ELMs above the quiescent background is measured to be the same order as that of the steady state background. As seen in the heat flux profiles the ELM particle fluxes are more balanced between inboard and outboard in DIII–D than in ASDEX-Upgrade. More important though is that the ELM flux spatial distribution is nearly centered on the quiescent profile. The time-averaged ELM particle flux spatial profile is very similar to the quiescent profile. The total integrated ELM particle flux cannot be correlated with the number of particles lost from the main plasma as the ejected particles must certainly recycle a number of times. An edge modeling code would aid in relating core plasma loss to surface particle fluxes.
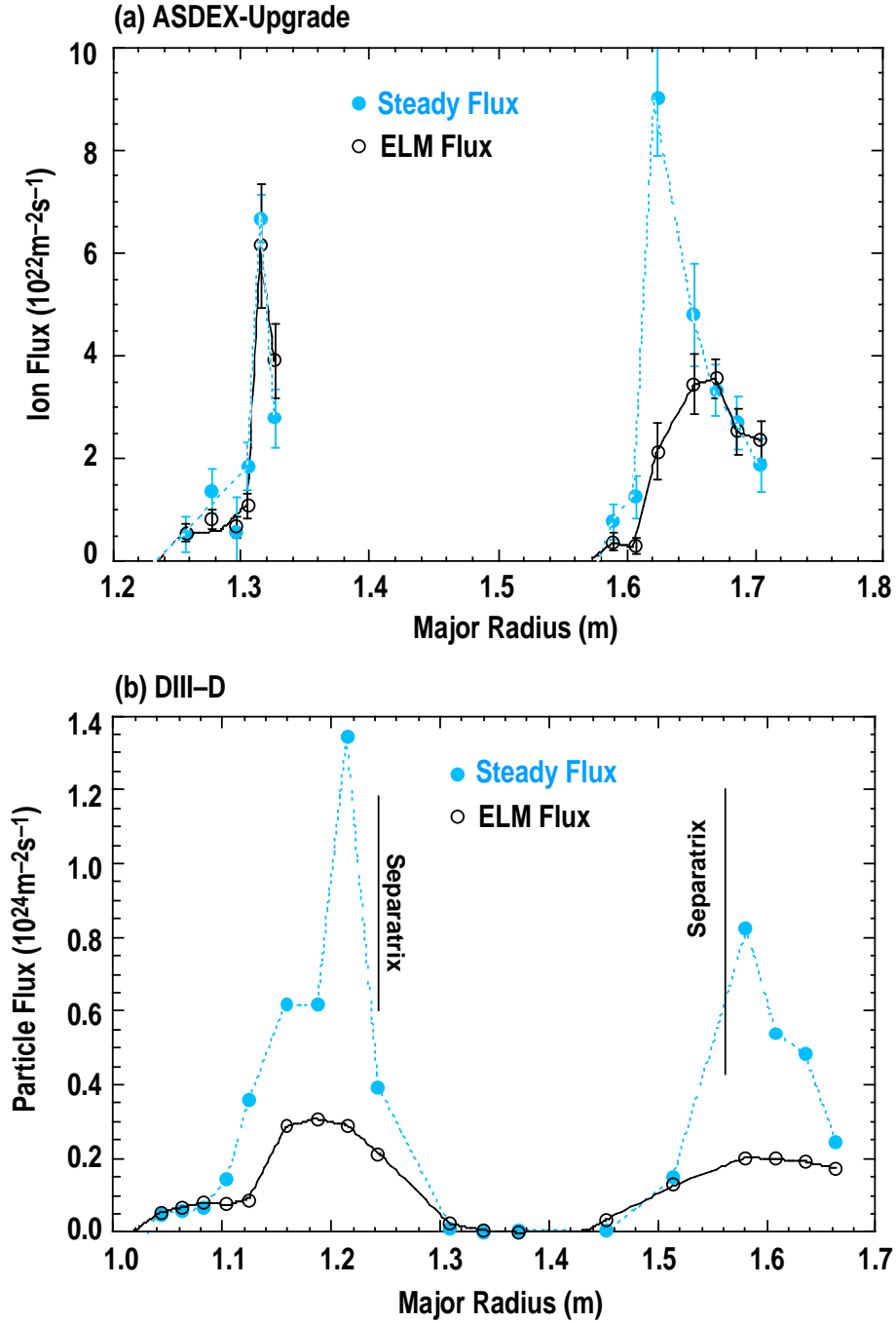
(a) ASDEX-Upgrade

(b) DIII–D

Fig. 4. The steady-state divertor plate particle fluxes between ELMs and the fluxes due to ELMs. The ELM flux is time-averaged over many ELMs with the steady-state quiescent level subtracted. The flux area for a) the ASDEX-Upgrade profiles is the divertor plate and for b) DIII–D the area perpendicular to the field lines

5. DISCUSSION

A number of similarities exist between Type I ELMs on DIII–D and ASDEX-Upgrade. On both tokamaks the energy loss per ELM varies from 6% to 2% of the main plasma stored energy as the input power increases above the H–mode power threshold. The uncertainty in this scaling is greatest at low power near the H–mode threshold. Also on both tokamaks energy lost from the core plasma is deposited on the divertor plates near the strike-points with a width somewhat greater than the heat flux between ELMs. However, this is in contrast to data from JT-60U [10] and particularly JET [11] that find ELM energy can fall significantly outside the separatrix and SOL. Toroidal asymmetry in the energy deposition is measured to be less than 1.5 on DIII–D. This is also consistent with the ASDEX-Upgrade data in that the ELM-to-ELM variation was less than 50% and there was no locking of the asymmetry to a particular toroidal angle on DIII–D. A final similarity is that the particle flux during an ELM is localized near the separatrix with a width similar to the quiescent phase between ELMs. Once again data from other tokamaks indicate that this deposition profile may not be universal.

A couple of significant differences still remain to be resolved. On ASDEX-Upgrade about 50% of the ELM energy loss is accounted for as divertor plate heat flux, while on DIII–D approximately all of the ELM energy is deposited on the divertor plate. One possibility is that while radiation accounts for only a small part of the ELM energy on DIII–D, it may be larger on ASDEX-Upgrade with its different parameters and geometry. Planned improvements to the ASDEX-Upgrade bolometer system will help answer this question. Another possibility is uncertainty in determining ELM energy loss and divertor flux in the two tokamaks. In order to determine main plasma ELM energy loss, the stored energy of the main plasma must be accurately determined on a time scale shorter than 1 ms. This requirement is just marginal on both tokamaks. The measurement of ELM divertor energy flux is also somewhat problematic in the conversion of surface temperature to heat flux. Though an energy constraint reduces the uncertainty in total ELM divertor energy, model assumptions and especially differences in the DIII–D and ASDEX-Upgrade IR diagnostic systems may lead to much of the difference.

A second difference in the data is the in/out asymmetry of the ELM energy flux. On ASDEX-Upgrade ≥75% of the ELM divertor plate energy falls on the inboard side, while on DIII–D the inboard side is only slightly higher than the outboard. This trend appears consistently throughout the data set studied. However, other DIII–D data not presented here has shown somewhat greater in/out asymmetry and data from JT-60U [10] and JET [11] also show much greater ELM energy fluxes to the inboard divertor. The degree of in/out asymmetry may be controlled by differences in geometry, divertor conditions or some other parameter.

With the data presented here one might estimate the energy flux due to a single ELM on ITER. From the scaling presented in Section 2 and plotted in Fig. 1 and an ITER surface area of 1250 m^2, toroidal field of 5.7 T, alpha heating power of 300 MW and a stored energy of 1200 MJ, a Type I ELM on ITER could lose ~3%, or 36 MJ of the main plasma energy. If all the energy is deposited evenly in a total divertor area of 10 m^2 then the energy density would be 3.6 MJ/m^2 for each ELM. This is not tolerable for the ITER divertor as significant erosion is expected to occur above a threshold of 1.5 MJ/m^2 if the energy is deposited in 1 ms [4]. The energy flux could also be a factor of 2 higher if there is a strong in/out asymmetry as indicated in some data. Toroidal asymmetries are not expected to make this value more than 50% higher. The ELM energy flux will be especially difficult to handle if it occurs outside the SOL as indicated on some tokamaks. The heat flux problem can be mitigated if the energy is deposited on a longer timescale of ~5ms or if much of the energy can be radiated. Future work should include a wider data set to include effects of detached divertor plasmas which may radiate a greater fraction of the ELM, plasma shape and edge plasma conditions which may effect ELM amplitude. Also the timescale of the ELM should be investigated for scaling to ITER plasmas and dimensions.

REFERENCES

[1]   H. Zohm, F. Ryter, C. Fuchs, A. Herrmann, M. Kaufmann, J. Neuhauser, N. Salmon, Plasma Physics and Controlled Fusion, 36 (4):A129

[2]   P. Gohil, M.A. Mahdavi, L.L. Lao, K.H. Burrell,M.S. Chu, J.C. DeBoo, C.L. Hsieh, N. Ohyabu, R.T. Snider, R.D. Stambaugh, R.E. Stockdale, Phys. Rev. Lett. 61 (14)

[3]   H. Zohm, T.H. Osborne, K.H. Burrell, M.S. Chu, E.J. Doyle, P. Gohil, D.N. Hill, L.L. Lao, A.W. Leonard, T. S. Taylor, A.D. Turnbull, Nucl. Fusion, 35 543 (1995)

[4]   K.J. Dietz, et. al., Proc. 15th Intl Conf. on Plasma Phys. and Contr. Nucl. Fusion Research, 1994, Seville Spain IAEA-CN-60/E-1-I-4

[5]   F. Ryter, accepted for publication in Nucl. Fusion

[6]   A. Herrmann, V. Rohde, M. Weinlich, M. Laux, G. Haas, A. Carlson, Proc. 22 EPS Conf. on Contr. Fusion and Plasma Phys., Bournemouth, 1995, III-241

[7]   D.N. Hill, R. Ellis, W. Ferguson, D.E. Perkins, T. Petrie and C. Baxi, Rev. Sci. Instr. 59 (1988) 1878

[8]   A. Herrmann, W. Junker, K. Gunther, S. Bosh, et., al., Plasma Phys. and Cont. Fusion 37 (1995) 17

[9]   T. E. Evans, C. J. Lasnier, D.N. Hill, A.W. Leonard, M.E. Fenstermacher, T.W. Petrie, and M.J. Schaffer, J. Nucl. Mater 220-222 (1995) 235

[10] K. Itami, N. Hosogane, N. Asakura, H. Kubo, S. Tsuji, M. Shimada, J. Nucl. Mater. 220-222 (1995) 203

[11] J. Lingertat, B. Alper, S. Ali-Arshad, et. al., Proc. 22 EPS Conf. on Contr. Fusion and Plasma Phys., Bournemouth, 1995, III-281

ACKNOWLEDGMENT